Model Hamiltonian Approach to the Infrared Intensities of Charged Conjugated π-Electron Systems

Hajime Torii*

Department of Chemistry, School of Science, The University of Tokyo, Bunkyo-ku, Tokyo 113-0033, Japan

Received: August 18, 1999; In Final Form: November 1, 1999

The changes in electronic structures generating large dipole derivatives for the CC stretches in charged conjugated (π-electron) hydrocarbon species are analyzed theoretically by deriving a relation between dipole derivatives and electric-field-induced changes in bond orders and by constructing a simple model Hamiltonian. The model Hamiltonian consists of the diagonal term representing the electric-field dependence of the energy on each site (carbon atom) and the off-diagonal term taken from the Su−Schrieffer−Heeger model. It is shown that the dipole derivatives calculated with the model Hamiltonian are in reasonable agreement with those obtained at the B3LYP/6-311G* level of density functional theory. It is concluded that the model Hamiltonian adequately describes the mechanisms that determine the signs and magnitudes of the dipole derivatives of the CC stretches in charged conjugated hydrocarbon species. For neutral species, the dipole derivatives of all the CC stretches are calculated to be zero by the model Hamiltonian. This is a consequence of the pairing theorem that holds for the molecular orbitals of the model Hamiltonian for alternant hydrocarbons and is consistent with the experimental results that the IR intensities are weak in the fingerprint region for neutral species. As examples of the application of the present approach, detailed analyses of the changes in the electronic structures generating dipole derivatives of the CC stretches are carried out for the radical cations of naphthalene, pentacene, biphenyl, perylene, and biphenylene, as well as for some related species.

1. Introduction

A noticeable feature in the infrared (IR) spectra of charged conjugated π-electron systems is that some bands in the fingerprint region (generally ranging from 1700 to 1000−900 cm^{-1}) have strong IR intensities.[1−13] In many cases, these IR bands are stronger by 1 or 2 orders of magnitude than the corresponding bands of the neutral species.[3,12,13] To understand this spectral feature, it is essential to characterize the vibrational patterns of the strongly IR-active modes and to clarify the mechanism that gives rise to the strong IR intensities.

In the case of charged linear polyenes and other related molecules, strong IR bands are induced by the vibrations along the bond-alternation coordinate,[3] in which adjacent CC bonds in a conjugated chain stretch and contract alternately. The mechanism giving rise to these strong IR bands may be most easily understood by considering two valence-bond resonance structures, in which an electric charge resides on either end of the conjugated chain. The locations of the electronic charge and the bond-alternation pattern in one of the resonance structures are opposite from those in the other. As a consequence, adjacent CC bonds stretch and contract alternately, and the electric charge moves from one end of the conjugated chain to the other, upon the transition between the two resonance structures. In other words, the electric charge moves through the conjugated chain by the vibration along the bond-alternation coordinate. This type of electron-vibration interaction may be formulated by using a two-state model Hamiltonian,[14,15] in which one vibrational degree of freedom (along the bond-alternation coordinate), two diabatic electronic states (corresponding to two valence-bond resonance structures), and the coupling between the two states are considered. However, in the cases of molecules with an intricate network of chemical bonds, a more general theoretical formulation is needed, since the vibrational patterns of the strongly IR-active modes cannot be anticipated from the molecular structures alone.

The radical ions of polycyclic aromatic hydrocarbons (PAHs) belong to such difficult cases. In a previous study,[16] the vibrational motions responsible for strong IR intensities (called *the intensity-carrying modes*) have been analyzed for the radical cations of PAHs by calculating the dipole derivatives with a density functional method and employing the doorway-state formalism.[17] It has been shown[16] that the CC stretches (rather than the CH bends) are mainly responsible for the strong IR intensities, and the vibrational patterns of the intensity-carrying modes and the directions of the dipole derivatives induced by them are closely related to the electronic structures, especially the phase relationship of the singly occupied molecular orbital (SOMO). This result suggests that a simple model, which takes only π electrons into account, may give good estimates of the dipole derivatives of these molecules, and that the relation between vibrational motions and the dipole derivatives induced by them may be examined with the model. Development of such a model will be useful for gaining a deep insight into the nature of the electron-vibration interactions in charged conjugated π-electron systems and their role in generating IR intensities.

In the present study, we first show the relation between dipole derivatives and electric-field-induced changes in bond orders. A simple model Hamiltonian is then constructed by incorporating the electric field dependence of the energy on each site (carbon atom) into the Su−Schrieffer−Heeger (SSH) model.[18,19] It is demonstrated that good estimates of the signs and

* Corresponding author. Phone: +81-3-5841-4329. Fax: +81-3-3818-4621. E-mail: torii@chem.s.u-tokyo.ac.jp.

10.1021/jp992910c CCC: $19.00
Published on Web 12/17/1999

magnitudes of dipole derivatives are obtained by such a simple model for the CC stretches in many charged conjugated hydrocarbon species.[20] The changes in electronic structures generating large dipole derivatives are analyzed. It is shown that the result of the present analysis rationalizes the concept of long-range and short-range charge fluxes, which is introduced in the previous study[16] to explain the vibrational motions responsible for strong IR intensities and the directions of the dipole derivatives generated by those vibrations.

2. Theory

A. Relation between Dipole Derivatives and Electric-Field-Induced Changes in Bond Orders. The dipole derivative with respect to the *m*th bond-stretching coordinate (R_m), denoted by $\partial\mu_k/\partial R_m$ ($k = x, y, z$), is related to a change in the potential energy gradient induced by an electric field as[21]

$$\frac{\partial \mu_k}{\partial R_m} = -\frac{\partial}{\partial E_k}\frac{\partial V}{\partial R_m} \tag{1}$$

where V is the potential energy of a given molecule, and E_k is an electric field in the k ($= x, y, z$) direction. An increase in the value of $\partial V/\partial R_m$ results in a decrease of the equilibrium bond length, and hence an increase in the π bond order (I_m), of the *m*th bond. It is therefore expected that $-\partial I_m/\partial E_k$ is closely related to, and has the same sign as, $\partial\mu_k/\partial R_m$.

We confine ourselves to the case of the CC stretches in conjugated π-electron systems containing no heteroatoms. A change in the π bond order of a CC bond by 1 is expected to induce a change in the equilibrium bond length by about 0.1 Å. This results in a change in the value of $\partial V/\partial R_m$ by about 0.6 mdyn or 0.07 au (at the equilibrium structure of the molecule unperturbed by the electric field), considering that a typical value of the CC stretching force constant is about 6 mdyn Å^{-1}. Therefore, it is considered that 1 au of $-\partial I_m/\partial E_k$ corresponds to 0.07 au or 0.35 D Å^{-1} of $\partial\mu_k/\partial R_m$.

In the present study, we use this relation to obtain estimates of $\partial\mu_k/\partial R_m$ from the values of $-\partial I_m/\partial E_k$ calculated by using the model Hamiltonian described below.

B. Model Hamiltonian. The model Hamiltonian used in this study is

$$H = H_{\mathrm{d}} + H_{\mathrm{od}} \tag{2}$$

in which the second term (the off-diagonal term) is expressed as

$$H_{\mathrm{od}} = \sum_{\substack{i<j \\ \text{(bonded)}}} \sum_{\sigma} [-t_0 + d(\rho_{ij} - \rho_{\mathrm{ref}})]\,(a_{i\sigma}^{\dagger}a_{j\sigma} + a_{j\sigma}^{\dagger}a_{i\sigma}) \tag{3}$$

where $a_{i\sigma}^{\dagger}$ is the creation operator of an electron of spin σ at site i (i.e., the ith carbon atom), $a_{i\sigma}$ is the corresponding annihilation operator, ρ_{ij} is the length of the bond connecting sites i and j, ρ_{ref} is the reference bond length (1.4 Å), t_0 is the reference value for the coupling constants between sites, and d stands for the dependence of the coupling constants on the bond lengths. The summation over i and j is taken for pairs of sites i and j within a specified distance (1.6 Å), i.e., for those connected by a chemical bond. This off-diagonal term is just the model Hamiltonian used by Su, Schrieffer, and Heeger (the SSH model)[18,19] for discussing the electronic and vibrational motions in polyacetylene. Only π electrons are explicitly considered in this Hamiltonian. The term $d(\rho_{ij} - \rho_{\mathrm{ref}})$ is introduced to consider the effects of the Peierls distortion or the Jahn−Teller distortion on the electronic structures. When $d = 0$, H_{od} is reduced to the Hückel Hamiltonian of π-electron systems. We assume $t_0 = 2.5$ eV and $d = 4.1$ eV Å^{-1}, which are considered to be typical values of these quantities.[18,19] The final results are not sensitive to the value of d, provided that the degeneracy of the orbitals related to the Peierls distortion or the Jahn−Teller distortion is sufficiently lifted.

The SSH model Hamiltonian is extended, as given in eq 2, by adding a diagonal term, which is expressed as

$$H_{\mathrm{d}} = \sum_{i,\sigma} e\mathbf{r}_i\mathbf{E}a_{i\sigma}^{\dagger}a_{i\sigma} \tag{4}$$

where $\mathbf{r}_i$ stands for the position of site i, $\mathbf{E}$ is an electric field (vector), and e is the elementary charge. Because of the existence of this diagonal term, the electronic structure depends on the electric field.

The molecular orbitals are calculated by solving this model Hamiltonian. The π bond order of the *m*th bond (which connects sites i and j) is expressed as

$$I_m = \sum_{p,\sigma} n_{p\sigma}\, c_{i,p\sigma}\, c_{j,p\sigma} \tag{5}$$

where $c_{i,p\sigma}$ is the coefficient of molecular orbital p with spin σ at site i, and $n_{p\sigma}$ is the occupation number (0 or 1). In the present study, the bond orders are calculated under finite electric field ($\pm 3 \times 10^{-4}$ au) and differentiated numerically to obtain $\partial I_m/\partial E_k$.

C. Contribution of Changes in Electronic Structures to Dipole Derivatives. The π bond order of the *m*th bond given in eq 5 is rewritten (by explicitly showing the electric field dependence of the quantities) as

$$I_m(\mathbf{E}) = \langle g(\mathbf{E})|\sum_{\sigma} a_{j\sigma}^{\dagger}a_{i\sigma}|g(\mathbf{E})\rangle \tag{6}$$

where $|g(\mathbf{E})\rangle$ is the electronic wave function of the ground electronic state evaluated under finite electric field $\mathbf{E}$. The electric field dependence of $I_m(\mathbf{E})$ originates from that of $|g(\mathbf{E})\rangle$ (and $\langle g(\mathbf{E})|$). To the first order in $\mathbf{E}$, $|g(\mathbf{E})\rangle$ is expanded as

$$|g(\mathbf{E})\rangle = |g_0\rangle + \sum_{k=x,y,z} |\delta_k\rangle E_k \tag{7}$$

where $|g_0\rangle$ is the unperturbed wave function of the ground electronic state. From eqs 6 and 7, we obtain

$$\frac{\partial I_m}{\partial E_k} = \langle g_0|\sum_{\sigma} a_{j\sigma}^{\dagger}\, a_{i\sigma}|\delta_k\rangle + \langle \delta_k|\sum_{\sigma} a_{j\sigma}^{\dagger}a_{i\sigma}|g_0\rangle \tag{8}$$

where both sides are evaluated at $\mathbf{E} = 0$. In this paper, all the electronic wave functions are taken to be real. Equation 8 is then rewritten as

$$\frac{\partial I_m}{\partial E_k} = \langle g_0|\sum_{\sigma} (a_{i\sigma}^{\dagger}a_{j\sigma} + a_{j\sigma}^{\dagger}a_{i\sigma})|\delta_k\rangle \tag{9}$$

Considering that $\langle g_0|\delta_k\rangle = 0$ is satisfied, $|\delta_k\rangle$ may be expanded by excited electronic configurations $|\nu_s\rangle$ (numbered by s) calculated at $\mathbf{E} = 0$. We obtain

$$\frac{\partial I_m}{\partial E_k} = \sum_{\mathrm{s}} f_{k,s}P_{ij,s} \tag{10}$$

where

$$f_{k,s} = \langle \nu_s | \delta_k \rangle = \frac{\partial}{\partial E_k} \langle \nu_s | g(\mathbf{E}) \rangle \quad (11)$$

represents the electric-field-induced mixing of excited electronic configurations into the ground electronic state, and

$$P_{ij,s} = \langle g_0 | \sum_{\sigma} (a_{i\sigma}^{\dagger} a_{j\sigma} + a_{j\sigma}^{\dagger} a_{i\sigma}) | \nu_s \rangle \quad (12)$$

is an element of the one-particle transition density matrix[22] between $|g_0\rangle$ and $|\nu_s\rangle$.

Since $a_{i\sigma}^{\dagger} a_{j\sigma} + a_{j\sigma}^{\dagger} a_{i\sigma}$ appearing in eq 12 is a one-electron operator, $P_{ij,s}$ vanishes if $|\nu_s\rangle$ is made by excitation of two or more electrons from $|g_0\rangle$. It is therefore concluded that only the mixing of one-electron excited configurations contributes to $\partial I_m/\partial E_k$, and hence to $\partial \mu_k/\partial R_m$, within the framework of the present theory. In eq 10, $f_{k,s}$ determines the magnitude of the mixing of $|\nu_s\rangle$, and $P_{ij,s}$ determines the relative signs and magnitudes of the bond-order changes arising from the mixing. The vibrational motions giving rise to large IR intensities may be analyzed by inspecting the signs and magnitudes of $P_{ij,s}$ for $|\nu_s\rangle$ having large values of $f_{k,s}$.

3. Validity of the Model

To see the validity of the model presented in section 2, dipole derivatives are calculated for the CC stretches in many charged conjugated hydrocarbon species by using the model and are compared with those calculated with a density functional method. The calculations are carried out for the pentadienyl cation, the heptatrienyl cation, and the radical cations of the following species: benzene, linear polyacenes ranging from naphthalene to heptacene, phenanthrene, chrysene, triphenylene, biphenyl, biphenylene, and [3]phenylene. Since all these species have no carbon atoms shared by three rings, it is feasible to define a nonredundant set of internal coordinates in the same way as in our previous studies[13,23,24] so that the dipole derivatives in the Cartesian coordinate system obtained from density functional calculations may be transformed to those in the internal coordinate system. The density functional calculations are carried out[25] at the B3LYP (Becke's three-parameter hybrid method[26] using the Lee−Yang−Parr correlation functional[27]) level with the 6-311G* basis set,[28] by using the Gaussian 94 program.[29] As shown in refs 12 and 13, the IR spectra calculated at the B3LYP level are in good agreement with the experimental results for many PAH radical ions. It is therefore expected that the calculations at the B3LYP level will provide sufficiently reliable values of dipole derivatives, which can be regarded as reference values to be compared with the dipole derivatives calculated with the model Hamiltonian. In the present study, the optimized structures obtained at the B3LYP/6-311G* level are used as input in the calculations based on the model Hamiltonian. However, the values of the dipole derivatives calculated with the model Hamiltonian do not depend sensitively on the structural parameters used.

The result is shown in Figure 1. It is seen that the dipole derivatives calculated with the model Hamiltonian are in reasonable agreement with those obtained at the B3LYP/6-311G* level of density functional theory. This result indicates that the model Hamiltonian adequately describes the mechanisms that determine the signs and magnitudes of the dipole derivatives of the CC stretches in charged conjugated hydrocarbon species. It is also demonstrated that the relation between $\partial \mu_k/\partial R_m$ and $\partial I_m/\partial E_k$ derived in section 2.A, expressed as $\partial \mu_k/\partial R_m \cong -0.07\ \partial I_m/\partial E_k$ in atomic units, is reasonable, although the coefficient in this relation (−0.07) is only roughly estimated as described in its derivation.

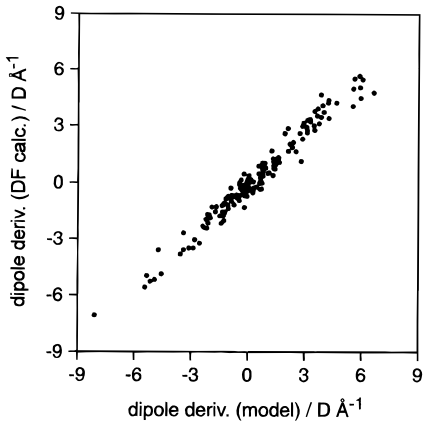

Figure 1. Comparison of the dipole derivatives of the CC stretches calculated by using the model Hamiltonian (eqs 2−4) with those calculated at the B3LYP/6-311G* level of density functional theory. Calculations are carried out for many cationic species listed in the text.

For the neutral molecules (in the ground electronic state) corresponding to all of the above charged species, the dipole derivatives of all the CC stretches are calculated to be zero with the present model Hamiltonian. This is in accord with the results obtained from experiments and from ab initio molecular orbital and density functional calculations that the IR intensities of the CC stretching bands are very weak in neutral species and are significantly enhanced upon ionization.[1−3,8−13]

From these results, we conclude that the model Hamiltonian may be used for detailed analyses of the nature of the electron-vibration interactions that generate large dipole derivatives for the CC stretches in charged conjugated π-electron systems.

4. Detailed Analyses of Some Illustrative Cases

In this section, we analyze the changes in electronic structures that generate large dipole derivatives for some positively charged conjugated hydrocarbon species as examples.

As shown in section 2.C, only the mixing of one-electron excited configurations contributes to electric-field-induced changes in bond orders, and hence to dipole derivatives. In general, various one-electron excited configurations $|\nu_s\rangle$ are mixed into the wave function $|g(\mathbf{E})\rangle$ upon applying electric field regardless of whether the molecule is neutral or charged. The dipole derivatives calculated with the present model Hamiltonian are zero for neutral species in the ground electronic state, because the contribution of the $\alpha_p \rightarrow \alpha_q$ excited configuration (made by excitation of one α electron from occupied orbital p to virtual orbital q) is exactly canceled by that of the $\beta_{N+1-q} \rightarrow \beta_{N+1-p}$ configuration, where N is the number of sites (i.e., the number of carbon atoms) in the molecule, and the contribution of the $\beta_p \rightarrow \beta_q$ configuration is canceled by that of the $\alpha_{N+1-q} \rightarrow \alpha_{N+1-p}$ configuration. This is a consequence of the pairing theorem[30] that holds for the molecular orbitals of the present model Hamiltonian for alternant hydrocarbons. In the case of a univalent radical cation with M α electrons and $M - 1$ β electrons (where $M = N/2$), only the contributions of the $\beta_p \rightarrow \beta_M$ and $\alpha_p \rightarrow \alpha_{M+1}$ configurations (referred to as the C-type configurations hereafter) remain after cancellation, because there is no longer a β electron on the Mth orbital. In the case of a closed-shell cationic species made by ionization of a neutral

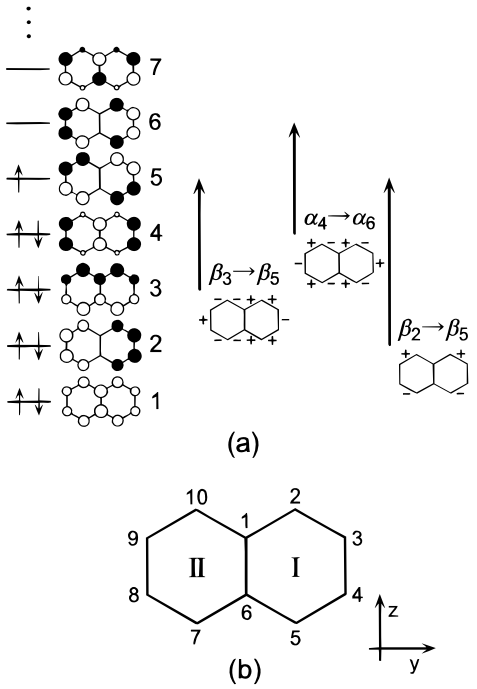

Figure 2. (a) The forms of orbitals 1−7, the occupation of α and β electrons in these orbitals, the electronic excitations involved in intensity-generating configurations, and the signs of the dipole derivatives generated by the mixing of these configurations calculated for the naphthalene radical cation. (b) The coordinate axes and the numbering of atoms and rings defined for this species.

radical, the contributions of the $\alpha_p \rightarrow \alpha_S$ and $\beta_p \rightarrow \beta_S$ configurations (where $S = (N + 1)/2$) are left after cancellation.

In the following, the dipole derivatives generated by the mixing of these types of excited electronic configurations are analyzed in detail.

A. Naphthalene Radical Cation and Related Species. For radical cations with highly symmetric structures, C-type configurations that may be mixed into $|g(\mathbf{E})\rangle$ are limited in number by symmetry. The lowest seven orbitals of the naphthalene radical cation (with D_{2h} symmetry) are shown on the left-hand side of Figure 2a.[31] The coordinate axes, together with the numbering of atoms and rings, are shown in Figure 2b. It is evident from the symmetry of each orbital that, among various C-type configurations, only the $\beta_3 \rightarrow \beta_5$, $\alpha_1 \rightarrow \alpha_6$, and $\alpha_4 \rightarrow \alpha_6$ configurations are mixed into $|g(E_y)\rangle$, and only the $\beta_2 \rightarrow \beta_5$ and $\alpha_5 \rightarrow \alpha_6$ configurations are mixed into $|g(E_z)\rangle$. Since $f_{y,s}$ is small for the $\alpha_1 \rightarrow \alpha_6$ configuration and $P_{ij,s}$ is zero for all the CC bonds for the $\alpha_5 \rightarrow \alpha_6$ configuration, only the mixing of the $\beta_3 \rightarrow \beta_5$, $\alpha_4 \rightarrow \alpha_6$, and $\beta_2 \rightarrow \beta_5$ configurations are important in generating dipole derivatives of the CC stretches in the naphthalene radical cation. It may be said that these excited configurations are *the intensity-generating configurations*.

Quantitative estimates of the dipole derivatives generated by the mixing of these intensity-generating configurations (equal to $-0.07 f_{k,s} P_{ij,s}$), as well as the values of $f_{k,s}$, are shown in Table 1. The signs of the dipole derivatives are depicted in Figure 2a.

By the mixing of the $\beta_3 \rightarrow \beta_5$ configuration (with a positive value of $f_{y,s}$), dipole derivatives in the $+y$ direction are generated for the stretching of the C_1C_2, C_2C_3, C_4C_5, and C_5C_6 bonds of ring I and the C_8C_9 bond of ring II, and those in the $-y$ direction are generated for the stretching of the rest of the CC bonds except the C_1C_6 bond. In other words, a large dipole derivative in the $+y$ direction is induced by a delocalized vibrational mode consisting of the stretching of the C_1C_2, C_2C_3, C_4C_5, and C_5C_6 bonds and the contraction of the C_3C_4 bond in ring I and the corresponding opposite-phase vibrations in ring II. The charge flux induced by this delocalized vibrational mode is derived from the change in the electronic structure occurring upon the mixing of the $\beta_3 \rightarrow \beta_5$ configuration. From the forms of orbitals 3 and 5 shown in Figure 2a, it is clear that the population of the unpaired electron shifts toward ring II by this mixing. As a result, the electric charge goes back and forth between rings I and II as the vibration proceeds in the delocalized vibrational mode. The concept of *long-range charge flux* introduced in ref 16 is therefore rationalized by this result.

By the mixing of the $\alpha_4 \rightarrow \alpha_6$ configuration (with a positive value of $f_{y,s}$), dipole derivatives in the $+y$ direction are generated for the stretching of the C_1C_2, C_3C_4, C_5C_6, C_7C_8, and C_9C_{10} bonds, and those in the $-y$ direction are generated for the stretching of the rest of the CC bonds except the C_1C_6 bond, as shown in Figure 2a. One may think that the dipole derivatives generated by this mixing in the $C_9-C_{10}-C_1-C_2-C_3$ part (and in the symmetry related $C_8-C_7-C_6-C_5-C_4$ part) are similar to those of the pentadienyl cation[15] in that the signs change alternately along the chain. However, as shown in Figure 3b, the signs of the dipole derivatives calculated for the latter are totally opposite to those in the former. This is because the forms of orbitals 4 and 6 in the $C_9-C_{10}-C_1-C_2-C_3$ part of the naphthalene radical cation are quite different from those of orbitals 2 and 3 of the pentadienyl cation, which are the orbitals involved in the intensity-generating configurations of this species. By contrast, the dipole derivatives generated in the $C_{10}-C_1-C_2$ part (and in the symmetry related $C_7-C_6-C_5$ part) of the naphthalene radical cation are indeed similar to those of the allyl cation shown in Figure 3a. In this case, the forms of the orbitals involved in the intensity-generating configurations are also similar.

TABLE 1: Contribution of the Mixing of Excited Electronic Configurations to the Dipole Derivatives $\partial\mu_k/\partial R_m$ ($k = y$ and z, in Units of D Å^{-1}) of the Naphthalene Radical Cation

	$\partial\mu_y/\partial R_m$			$\partial\mu_z/\partial R_m$
coordinate	total	$\beta_3 \rightarrow \beta_5$ (38.7)[a]	$\alpha_4 \rightarrow \alpha_6$ (13.5)	$\beta_2 \rightarrow \beta_5$ (=total) (18.8)
R_1 (C_1C_2 stretch)	2.871	2.020	0.841	0.000
R_2 (C_2C_3 stretch)	1.580	2.402	−0.823	1.649
R_3 (C_3C_4 stretch)	−0.229	−1.215	0.992	0.000
R_4 (C_1C_6 stretch)	0.000	0.000	0.000	0.000

[a] The value of $f_{k,s}$ (eq 11) in atomic units.

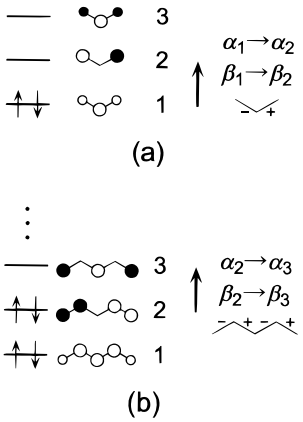

Figure 3. The forms of orbitals 1−3, the occupation of α and β electrons in these orbitals, the electronic excitations involved in intensity-generating configurations, and the signs of the dipole derivatives generated by the mixing of these configurations calculated for (a) the allyl cation and (b) the pentadienyl cation.

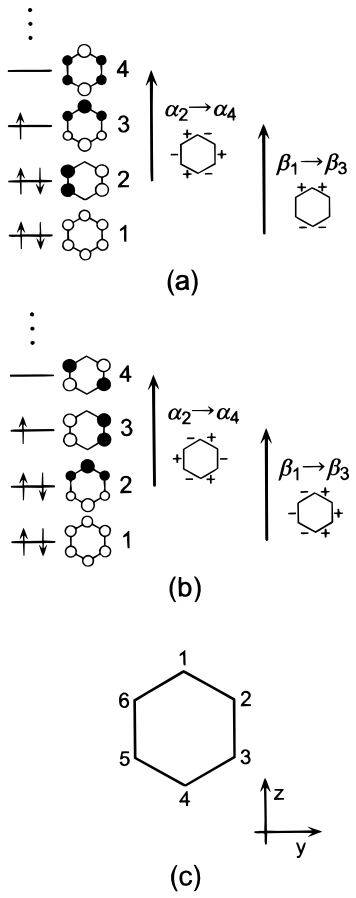

Figure 4. The forms of orbitals 1−4, the occupation of α and β electrons in these orbitals, the electronic excitations involved in intensity-generating configurations, and the signs of the dipole derivatives generated by the mixing of these configurations calculated for (a) structure A and (b) structure B of the benzene radical cation. (c) The coordinate axes and the numbering of atoms defined for these species.

To gain more insight into the signs of the dipole derivatives generated by the mixing of the $\alpha_4 \rightarrow \alpha_6$ configuration in the naphthalene radical cation, dipole derivatives and changes in electronic structures are examined for the benzene radical cation. Since neutral benzene has a degenerate pair of highest occupied molecular orbitals (HOMOs), there are two Jahn−Teller distorted structures for the benzene radical cation, denoted by structures A and B hereafter, depending on the HOMO of the neutral from which an electron is removed. The molecular orbitals calculated for these two structures (with D_{2h} symmetry) are shown on the left-hand side of parts a and b of Figure 4. As discussed in ref 16, comparison of the forms of the SOMOs suggests that structure A of the benzene radical cation may be regarded as building blocks constituting the naphthalene radical cation. We therefore discuss only the properties of structure A in this context. The intensity-generating configurations and the dipole derivatives generated by them are shown in Table 2 and on the right-hand side of Figure 4a. The coordinate axes and the numbering of atoms are shown in Figure 4c. It is seen that, among various C-type configurations, only the $\alpha_2 \rightarrow \alpha_4$ configuration is relevant to the dipole derivatives in the $\pm y$ direction ($\partial\mu_y/\partial R_m$). Other C-type configurations are not mixed into $|g(E_y)\rangle$ by symmetry.

By comparing the forms of the orbitals shown in Figure 2a and in Figure 4a, it is noticed that the change in the electronic structure induced in each ring of the naphthalene radical cation by the mixing of the $\alpha_4 \rightarrow \alpha_6$ configuration is very similar to that induced in the benzene radical cation structure A by the mixing of the $\alpha_2 \rightarrow \alpha_4$ configuration. This similarity suggests that charge flux is generated within each ring of the former in the same way as in the latter. As shown in Figures 2a and 4a, the signs of the dipole derivatives generated in each ring of the former are also the same as those in the latter. The concept of *short-range charge flux* introduced in ref 16 is therefore rationalized by this result.

TABLE 2: Contribution of the Mixing of Excited Electronic Configurations to the Dipole Derivatives $\partial\mu_k/\partial R_m$ ($k = y$ and z, in Units of D Å^{-1}) of the Benzene Radical Cation

	$\partial\mu_y/\partial R_m$			$\partial\mu_z/\partial R_m$	
coordinate	total	$\beta_1 \rightarrow \beta_3$ (18.8)[a,b]	$\alpha_2 \rightarrow \alpha_4$ (7.3)[a,c]	total	$\beta_1 \rightarrow \beta_3$ (18.8)[a,d]
		Structure A			
R_1 (C_1C_2 stretch)	−0.750		−0.750	2.330	2.330
R_2 (C_2C_3 stretch)	0.725		0.725	0.000	0.000
		Structure B			
R_1 (C_1C_2 stretch)	2.105	1.371	0.734	0.000	
R_2 (C_2C_3 stretch)	1.891	2.650	-0.759	0.000	

[a] The value of $f_{k,s}$ (eq 11) in atomic units. [b] For structure B. [c] For both structures A and B. [d] For structure A.

As shown in Table 1 and in Figure 2a, dipole derivatives in the $\pm z$ direction ($\partial\mu_z/\partial R_m$) are generated in the naphthalene radical cation by the mixing of the $\beta_2 \rightarrow \beta_5$ configuration. The change in the electronic structure induced in each ring by this mixing is similar to that induced by the mixing of the $\beta_1 \rightarrow \beta_3$ configuration in the benzene radical cation structure A, which is shown in Figure 4a. In this respect, $\partial\mu_z/\partial R_m$ in the naphthalene radical cation is also generated by the mechanism of short-range charge flux.

The picture obtained above on the mechanisms that generate large dipole derivatives in the naphthalene radical cation also holds for the radical cations of longer linear polyacenes. We take the case of the pentacene radical cation as an example. Among various C-type configurations, only the $\beta_{10} \rightarrow \beta_{11}$ and $\alpha_9 \rightarrow \alpha_{12}$ configurations are of primary importance in generating dipole derivatives in the $\pm y$ direction ($\partial\mu_y/\partial R_m$). The signs of the dipole derivatives and the orbitals involved in these excited configurations are shown in Figure 5a. The coordinate axes and the numbering of rings are shown in Figure 5b.

It is evident from the forms of the orbitals that the mixing of the $\alpha_9 \rightarrow \alpha_{12}$ configuration (with a positive value of $f_{y,s}$) induces a change in the electronic structure of each ring in the pentacene radical cation in the same way as the mixing of the $\alpha_4 \rightarrow \alpha_6$ configuration in the naphthalene radical caiton. Short-range charge flux is therefore generated by this mixing. In contrast, by the mixing of the $\beta_{10} \rightarrow \beta_{11}$ configuration (with a positive value of $f_{y,s}$), the population of the unpaired electron becomes smaller in rings I and II and larger in rings IV and V. This population change means that long-range charge flux is generated. The change in the electronic structure occurring in ring III by the mixing of the $\beta_{10} \rightarrow \beta_{11}$ configuration is rather difficult to interpret. By considering the upper and lower halves of this ring separately, it may be said that this electronic structural change is similar to that induced by the mixing of the $\alpha_9 \rightarrow \alpha_{12}$ configuration. In this respect, short-range charge flux is generated in ring III by the mixing of the $\beta_{10} \rightarrow \beta_{11}$ configuration as well as by the mixing of the $\alpha_9 \rightarrow \alpha_{12}$ configuration.

In rings I and V, the dipole derivatives generated by the mixing of the $\beta_{10} \rightarrow \beta_{11}$ configuration are larger in magnitude than those generated by the mixing of the $\alpha_9 \rightarrow \alpha_{12}$ configuration, although these two contributions partially cancel each other. Therefore, the dipole derivatives $\partial\mu_y/\partial R_m$ in rings I and

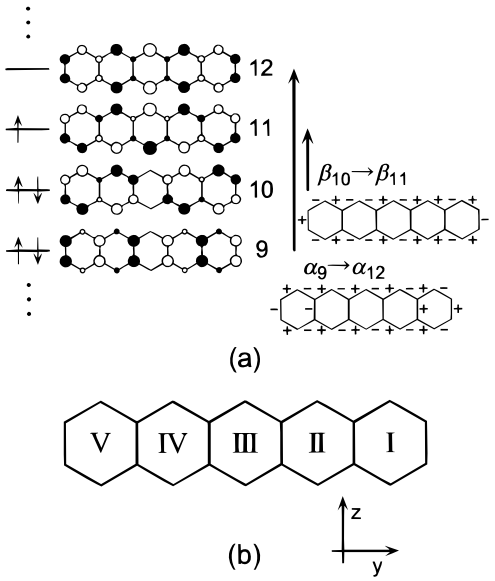

Figure 5. (a) The forms of orbitals 9−12, the occupation of α and β electrons in these orbitals, the electronic excitations involved in intensity-generating configurations, and the signs of the dipole derivatives generated by the mixing of these configurations calculated for the pentacene radical cation. (b) The coordinate axes and the numbering of rings defined for this species.

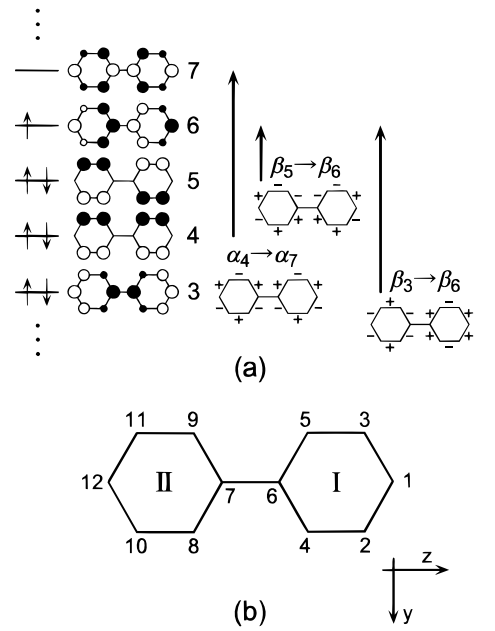

Figure 6. (a) The forms of orbitals 3−7, the occupation of α and β electrons in these orbitals, the electronic excitations involved in intensity-generating configurations, and the signs of the dipole derivatives generated by the mixing of these configurations calculated for the biphenyl radical cation. (b) The coordinate axes and the numbering of atoms and rings defined for this species.

V are mainly induced by the mechanism of long-range charge flux. This result is consistent with that obtained in ref 16.

B. Biphenyl Radical Cation. As another type of species made by connecting two benzene rings, over which electronic and vibrational excitations are delocalized, the biphenyl radical cation is selected as an example.

The forms of several important molecular orbitals of the biphenyl radical cation (with D_{2h} symmetry) are shown on the left-hand side of Figure 6a. (Orbitals 4 and 5 are degenerate for the present model Hamiltonian.) The coordinate axes, together with the numbering of atoms and rings, are shown in Figure 6b. It is derived from the symmetry of each orbital that, among various C-type configurations, only the $\beta_5 \rightarrow \beta_6$ and $\alpha_4 \rightarrow \alpha_7$ configurations are mixed into $|g(E_y)\rangle$, and only the $\beta_3 \rightarrow \beta_6$, $\beta_1 \rightarrow \beta_6$, $\alpha_2 \rightarrow \alpha_7$, and $\alpha_6 \rightarrow \alpha_7$ configurations are mixed into $|g(E_z)\rangle$. Among these, $f_{z,s}$ is very small for the $\alpha_2 \rightarrow \alpha_7$ configuration, and $P_{ij,s}$ is zero for all the CC bonds for the $\alpha_6 \rightarrow \alpha_7$ configuration. The dipole derivatives originating from the mixing of the other four configurations are shown in Table 3. The signs of the dipole derivatives (except those relevant to the $\beta_1 \rightarrow \beta_6$ configuration, for which $f_{z,s}$ is small) are depicted on the right-hand side of Figure 6a.

TABLE 3: Contribution of the Mixing of Excited Electronic Configurations to the Dipole Derivatives $\partial\mu_k/\partial R_m$ ($k = y$ and z, in Units of D Å^{-1}) of the Biphenyl Radical Cation

	$\partial\mu_y/\partial R_m$			$\partial\mu_z/\partial R_m$		
coordinate	total	$\beta_5 \rightarrow \beta_6$ (15.4)[a]	$\alpha_4 \rightarrow \alpha_7$ (9.0)	total	$\beta_3 \rightarrow \beta_6$ (66.1)	$\beta_1 \rightarrow \beta_6$ (2.7)
R_1 (C_1C_2 stretch)	−1.213	−0.766	−0.447	3.994	3.859	0.112
R_2 (C_2C_4 stretch)	0.794	0.313	0.481	−2.170	−2.107	−0.027
R_3 (C_4C_6 stretch)	0.282	0.677	−0.395	3.124	3.330	−0.218
R_4 (C_6C_7 stretch)	0.000	0.000	0.000	0.000	0.000	0.000

[a] The value of $f_{k,s}$ (eq 11) in atomic units.

The forms of orbitals 5 and 6 in each ring of the biphenyl radical cation are most similar to those of orbitals 2 and 3 of the benzene radical cation structure A. However, the $\beta_2 \rightarrow \beta_3$ configuration is not mixed into $|g(E_y)\rangle$ in the benzene radical cation because of the D_{2h} symmetry of its structure. The $\beta_5 \rightarrow \beta_6$ configuration is mixed into $|g(E_y)\rangle$ in the biphenyl radical cation because the $+z$ side of each ring is not equivalent to the $-z$ side. In contrast, the change in the electronic structure induced in each ring of the biphenyl radical cation by the mixing of the $\alpha_4 \rightarrow \alpha_7$ configuration is similar to that induced in the benzene radical cation structure A by the mixing of the $\alpha_2 \rightarrow \alpha_4$ configuration. The signs of the dipole derivatives generated in each ring of the former are also the same as those in the latter. Therefore, these dipole derivatives are explained by the mechanism of short-range charge flux.

As shown in Table 3, the dipole derivatives in the $\pm z$ direction ($\partial\mu_z/\partial R_m$) are almost totally generated by the mixing of the $\beta_3 \rightarrow \beta_6$ configuration. The forms of orbitals 3 and 6 shown in Figure 6a indicate that the population of the unpaired electron shifts toward ring II by this mixing (with a positive value of $f_{z,s}$). Consequently, the electric charge goes back and forth between rings I and II as the vibration proceeds in a delocalized vibrational mode consisting of the stretching of the C_1C_2, C_1C_3, C_4C_6, C_5C_6, C_8C_{10}, and C_9C_{11} bonds and the contraction of the rest of the CC bonds except the C_6C_7 bond. This result indicates that $\partial\mu_z/\partial R_m$ of the biphenyl radical cation are explained by the mechanism of long-range charge flux.

It has been shown[32] that strong electronic absorption bands of the biphenyl radical cation are observed at 14 200 and 25 800 cm^{-1}. These two bands arise from the $1^2B_{3u} \leftarrow 1^2B_{2g}$ and $2^2B_{3u} \leftarrow 1^2B_{2g}$ electronic transitions, and both the 1^2B_{3u} and 2^2B_{3u} electronic states contain large contributions from the $\beta_3 \rightarrow \beta_6$ and $\alpha_6 \rightarrow \alpha_7$ configurations.[33] In a previous study,[34] it is proposed that the vibronic interactions associated with both the $1^2B_{3u} \leftarrow 1^2B_{2g}$ and $2^2B_{3u} \leftarrow 1^2B_{2g}$ electronic transitions are effective in generating dipole derivatives in the $\pm z$ direction. The result of the present study indicates that only the $\beta_3 \rightarrow \beta_6$ configuration is important in generating those dipole derivatives.

C. Perylene Radical Cation. As an example of PAH radical cations extended in two dimensions, the case of the perylene radical cation is discussed in this subsection.

TABLE 4: Contribution of the Mixing of Excited Electronic Configurations to the Dipole Derivatives $\partial\mu_k/\partial R_m$ ($k = y$ and z, in Units of D Å^{-1}) of the Perylene Radical Cation

	$\partial\mu_y/\partial R_m$				$\partial\mu_z/\partial R_m$			
coordinate	total	$\beta_6 \rightarrow \beta_{10}$ (40.3)[a]	$\beta_8 \rightarrow \beta_{10}$ (18.9)	$\alpha_7 \rightarrow \alpha_{11}$ (17.2)	total	$\beta_9 \rightarrow \beta_{10}$ (62.5)	$\beta_3 \rightarrow \beta_{10}$ (2.8)	$\alpha_5 \rightarrow \alpha_{11}$ (1.7)
R_1 (C_1C_2 stretch)	2.013	1.540	−0.191	0.596	0.000	0.000	0.000	0.000
R_2 (C_2C_3 stretch)	−0.204	−0.356	0.685	−0.556	2.793	2.657	0.087	0.049
R_3 (C_3C_4 stretch)	0.277	0.056	−0.435	0.680	−1.885	−1.777	−0.032	−0.075
R_4 (C_4C_5 stretch)	1.670	1.756	0.263	−0.383	1.888	2.018	−0.149	0.018
R_5 (C_5C_6 stretch)	1.121	0.091	0.674	0.392	0.000	0.000	0.000	0.000
R_6 (C_1C_6 stretch)	0.000	0.000	0.000	0.000	0.000	0.000	0.000	0.000
R_7 (C_5C_{12} stretch)	−1.784	−1.139	−0.568	0.003	0.000	0.000	0.000	0.000

[a] The value of $f_{k,s}$ (eq 11) in atomic units.

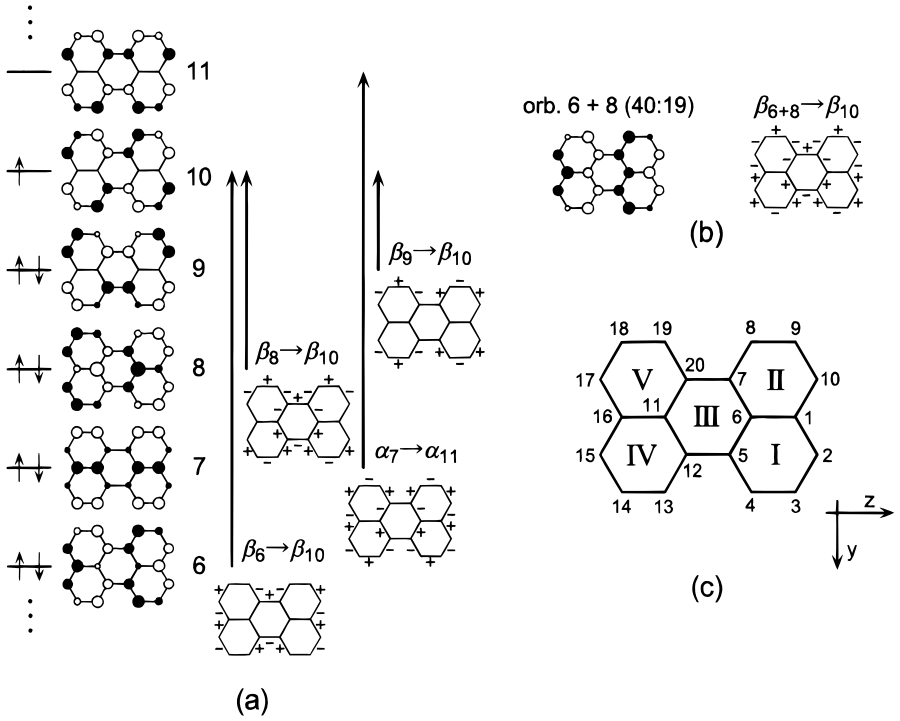

Figure 7. (a) The forms of orbitals 6−11, the occupation of α and β electrons in these orbitals, the electronic excitations involved in intensity-generating configurations, and the signs of the dipole derivatives generated by the mixing of these configurations calculated for the perylene radical cation. (b) The form of the linear combination of orbitals 6 and 8 taken with the ratio of 40:19, and the signs of the dipole derivatives generated by the mixing of the $\beta_{6+8} \rightarrow \beta_{10}$ configuration. (c) The coordinate axes and the numbering of atoms and rings defined for this species.

The dipole derivatives generated by the mixing of important excited configurations are shown in Table 4 and in Figure 7a, together with the forms of the molecular orbitals involved. The coordinate axes and the numbering of atoms and rings are shown in Figure 7c. The dipole derivatives in the $\pm y$ direction ($\partial\mu_y/\partial R_m$) are mainly generated by the mixing of the $\beta_6 \rightarrow \beta_{10}$, $\beta_8 \rightarrow \beta_{10}$, and $\alpha_7 \rightarrow \alpha_{11}$ configurations, and those in the $\pm z$ direction ($\partial\mu_z/\partial R_m$) are mainly generated by the mixing of the $\beta_9 \rightarrow \beta_{10}$ configuration.

The signs of the dipole derivatives generated by the mixing of the $\alpha_7 \rightarrow \alpha_{11}$ configuration are most easily understood by considering rings I and II as a group and rings IV and V as another. By comparing the forms of the orbitals shown in Figure 7a with those in Figure 2a, it is seen that the change in the electronic structure of each group occurring upon this mixing is very similar to that induced in the naphthalene radical cation by the mixing of the $\alpha_4 \rightarrow \alpha_6$ configuration. The signs of the dipole derivatives are also the same between these two cases. Following the discussion given in section 4.A, these dipole derivatives are explained by the mechanism of short-range charge flux.

The above grouping of rings is also useful for understanding the dipole derivatives generated by the mixing of the $\beta_6 \rightarrow \beta_{10}$ and $\beta_8 \rightarrow \beta_{10}$ configurations. The change in the electronic structure induced in each group of rings by the mixing of these two configurations is most easily seen by taking a linear combination of orbitals 6 and 8 with the ratio of 40:19, considering that the two configurations are mixed into $|g(E_y)\rangle$ in this ratio as shown in Table 4 (as the values of $f_{y,s}$). The form of this combined orbital and the signs of the generated dipole derivatives (the sum of the contributions from the $\beta_6 \rightarrow \beta_{10}$ and $\beta_8 \rightarrow \beta_{10}$ configurations) are shown in Figure 7b. It is seen that the change in the electronic structure induced in each group of rings by the $\beta_{6+8} \rightarrow \beta_{10}$ excitation is similar to that induced by the $\beta_3 \rightarrow \beta_5$ excitation in the naphthalene radical cation. It is therefore considered, following the discussion given in section 4.A, that (the fraction of) the unpaired electron goes back and forth between rings I and II and between rings IV and V as the vibration proceeds by the mixing of the $\beta_6 \rightarrow \beta_{10}$ and $\beta_8 \rightarrow \beta_{10}$ configurations in the perylene radical cation. The change in the electronic structure of ring III induced by the $\beta_{6+8} \rightarrow \beta_{10}$ excitation is explained in a different way. By comparing

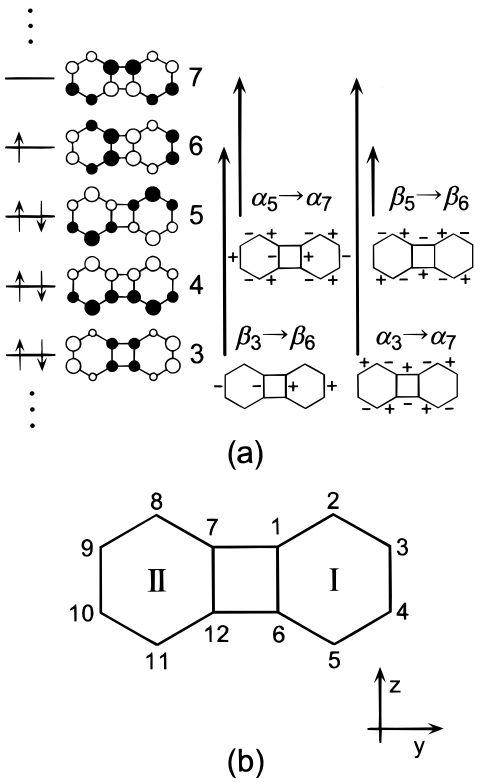

Figure 8. (a) The forms of orbitals 3−7, the occupation of α and β electrons in these orbitals, the electronic excitations involved in intensity-generating configurations, and the signs of the dipole derivatives generated by the mixing of these configurations calculated for the biphenylene radical cation. (b) The coordinate axes and the numbering of atoms and rings defined for this species.

parts a and b of Figure 7 with part b of Figure 4, it is noticed that this electronic structural change is similar to that induced by the $\alpha_2 \rightarrow \alpha_4$ excitation in the benzene radical cation structure B. Charge flux is therefore generated within ring III, and (the fraction of) the unpaired electron goes back and forth between the C_5C_{12} and C_7C_{20} bonds. Summarizing the above discussion, it may be said that the dipole derivatives depicted in Figure 7b are induced by the mechanisms of long-range and short-range charge fluxes.

By contrast, the dipole derivatives in the $\pm z$ direction ($\partial\mu_z/\partial R_m$) calculated for the perylene radical cation are reasonably well explained by adopting a different way of grouping of rings: rings I and IV connected by the C_5C_{12} bond as one group, and rings II and V connected by the C_7C_{20} bond as another. By comparing Figure 7a with Figure 6a, it is noticed that the change in the electronic structure induced in each group of rings by the $\beta_9 \rightarrow \beta_{10}$ excitation is similar to that induced by the $\beta_3 \rightarrow \beta_6$ excitation in the biphenyl radical cation. It is derived from this similarity that the dipole derivatives in the $\pm z$ direction in both cases are generated by a common mechanism, i.e., by the mechanism of long-range charge flux.

The above discussion demonstrates how the information obtained for small molecules may be used in analyses of larger molecules. It is expected that the electron-vibration interactions in many large systems may be discussed by considering (groups of) benzene rings as building blocks.

D. Biphenylene Radical Cation. Since biphenylene consists of two benzene rings (connected by two CC bonds) arranged side by side, as shown in Figure 8, one may guess that the dipole derivatives of the CC stretches in the biphenylene radical cation are similar to those in the naphthalene radical cation. However, as shown below, the dipole derivatives are significantly different, even in their signs, between the two cases because of the difference in their electronic structures.

TABLE 5: Contribution of the Mixing of Excited Electronic Configurations to the Dipole Derivatives $\partial\mu_k/\partial R_m$ ($k = y$ and z, in Units of D Å^{-1}) of the Biphenylene Radical Cation

	$\partial\mu_y/\partial R_m$			$\partial\mu_z/\partial R_m$		
coordinate	total	$\beta_3 \rightarrow \beta_6$ (42.6)[a]	$\alpha_5 \rightarrow \alpha_7$ (17.1)	total	$\beta_5 \rightarrow \beta_6$ (16.1)	$\alpha_3 \rightarrow \alpha_7$ (−8.7)
R_1 (C_1C_2 stretch)	−0.851	−0.131	−0.771	0.752	1.003	−0.256
R_2 (C_2C_3 stretch)	0.577	−0.373	0.967	−0.235	−0.529	0.311
R_3 (C_3C_4 stretch)	2.937	3.780	−0.808	0.000	0.000	0.000
R_4 (C_1C_6 stretch)	3.476	2.682	0.692	0.000	0.000	0.000
R_5 (C_1C_7 stretch)	0.000	0.000	0.000	−0.057	−0.653	0.545

[a] The value of $f_{k,s}$ (eq 11) in atomic units.

The forms of some important molecular orbitals of the biphenylene radical cation are shown on the left-hand side of Figure 8a. By comparing with parts a and b of Figure 4, it is clearly seen that the SOMO of the biphenylene radical cation is similar to that of structure B rather than structure A of the benzene radical cation. By contrast, as noted in section 4.A, the SOMO of the naphthalene radical cation is similar to that of structure A of the benzene radical cation. In this respect, the electronic structure is different between the radical cations of biphenylene and naphthalene.

The important intensity-generating electronic configurations and the dipole derivatives generated by the mixing of these configurations are shown in Table 5 and on the right-hand side of Figure 8a. The coordinate axes and the numbering of atoms and rings are shown in Figure 8b. It is seen that dipole derivatives in the $\pm y$ direction ($\partial\mu_y/\partial R_m$) are large and positive for the C_3C_4 and C_1C_6 stretches (and negative for the stretching of the symmetry related C_7C_{12} and C_9C_{10} bonds), and they primarily originate from the mixing of the $\beta_3 \rightarrow \beta_6$ configuration. The forms of the orbitals shown in Figure 8a indicate that the unpaired electron goes back and forth between rings I and II as the vibration proceeds by this mixing. The electronic structural change induced by the $\alpha_5 \rightarrow \alpha_7$ excitation is similar to that induced by the $\alpha_2 \rightarrow \alpha_4$ excitation in the benzene radical cation structure B. The mixing of this excited configuration generates short-range charge flux, but the dipole derivatives generated by this mixing are small in magnitude as shown in Table 5. It is therefore concluded that $\partial\mu_y/\partial R_m$ of the biphenylene radical cation are primarily explained by the mechanism of long-range charge flux.

Although $\partial\mu_y/\partial R_m$ of the naphthalene radical cation are also induced mainly by the mechanism of long-range charge flux as discussed in section 4.A, the signs and magnitudes of the generated dipole derivatives are significantly different between the two radical cations. In the case of the naphthalene radical cation, the values of $\partial\mu_y/\partial R_m$ are large and positive for the C_1C_2 and C_2C_3 stretches and negative (but small) for the C_3C_4 stretch, as shown in Table 1. However, in the case of the biphenylene radical cation, the values of $\partial\mu_y/\partial R_m$ are large and positive for the C_3C_4 and C_1C_6 stretches and small for the C_1C_2 and C_2C_3 stretches. The present analysis clearly shows that significantly different dipole derivatives are calculated for these two cases because their electronic structures are different.

The dipole derivatives in the $\pm z$ direction ($\partial\mu_z/\partial R_m$) of the biphenylene radical cation are generated by the mixing of the $\beta_5 \rightarrow \beta_6$ and $\alpha_3 \rightarrow \alpha_7$ configurations. However, the contributions of these configurations partially cancel each other, resulting in small values of $\partial\mu_z/\partial R_m$ as shown in Table 5 and Figure 8a. This result is reasonable in that the electronic structure of each

ring in the biphenylene radical cation is similar to that of structure B of the benzene radical cation, and no nonzero values of $\partial\mu_z/\partial R_m$ are calculated for the latter within the framework of the present theory.

5. Conclusion

The conclusions obtained in the present study may be summarized as follows. (1) For many charged conjugated hydrocarbon species, good estimates of the dipole derivatives ($\partial\mu_k/\partial R_m$) of the CC stretches are obtained from the electric-field-induced changes in bond orders ($\partial I_m/\partial E_k$) calculated by using the model Hamiltonian given in eqs 2−4. The model Hamiltonian adequately describes the mechanisms that determine the signs and magnitudes of the dipole derivatives of the CC stretches in charged conjugated hydrocarbon species. (2) Because $a_{i\sigma}^{\dagger}a_{j\sigma} + a_{j\sigma}^{\dagger}a_{i\sigma}$ appearing in eq 12 is a one-electron operator, only the mixing of one-electron excited configurations contributes to $\partial I_m/\partial E_k$, and hence to $\partial\mu_k/\partial R_m$, within the framework of the present theory. (3) Although various one-electron excited configurations $|\nu_s\rangle$ are mixed into $|g(\mathbf{E})\rangle$, contributions to $\partial\mu_k/\partial R_m$ from many configurations cancel each other because of the pairing theorem. As a result, the dipole derivatives of all the CC stretches of neutral species in the ground electronic state are calculated to be zero by the present model Hamiltonian. In the case of a univalent radical cation, only the contributions from the C-type configurations (defined at the beginning of section 4) remain after cancellation. (4) For the molecules treated in the present study, the dipole derivatives of the CC stretches are mainly generated by the mixing of a few excited configurations. The analysis of the change in the electronic structure occurring upon the mixing of each configuration and the dipole derivatives generated by this mixing supports the concept of long-range and short-range charge fluxes, which is introduced in ref 16 to explain the vibrational motions responsible for strong IR intensities and the directions of the dipole derivatives generated by those vibrations.

Because of the simplicity of the model Hamiltonian given in eqs 2−4, the model Hamiltonian approach presented in this paper may be applied to many large charged conjugated π-electron systems. It is hoped that the present theory and the results obtained for the examples given in section 4 will be of help in obtaining insight into the nature of the electron-vibration interactions in conjugated π-electron systems.

References and Notes

(1) Fincher, C. R., Jr.; Ozaki, M.; Heeger, A. J.; MacDiarmid, A. G. *Phys. Rev. B* **1979**, *19*, 4140.

(2) Harada, I.; Furukawa, Y.; Tasumi, M.; Shirakawa, H.; Ikeda, S. *J. Chem. Phys.* **1980**, *73*, 4746.

(3) Gussoni, M.; Castiglioni, C.; Zerbi, G. In *Spectroscopy of Advanced Materials*; Clark, R. J. H., Hester, R. E., Eds.; Advances in Spectroscopy; Wiley: New York, 1991; Vol. 19, p 251.

(4) Lussier, L. S.; Sandorfy, C.; Le-Thanh, H.; Vocelle, D. *Photochem. Photobiol.* **1987**, *45*, 801.

(5) Lussier, L. S.; Sandorfy, C.; Le-Thanh, H.; Vocelle, D. *J. Phys. Chem.* **1987**, *91*, 2282.

(6) Masuda, S.; Torii, H.; Tasumi, M. *J. Phys. Chem.* **1996**, *100*, 15335.

(7) Furuya, K.; Inagaki, Y.; Torii, H.; Furukawa, Y.; Tasumi, M. *J. Phys. Chem. A* **1998**, *102*, 8413.

(8) Szczepanski, J.; Roser, D.; Personette, W.; Eyring, M.; Pellow, R.; Vala, M. *J. Phys. Chem.* **1992**, *96*, 7876.

(9) Vala, M.; Szczepanski, J.; Pauzat, F.; Parisel, O.; Talbi, D.; Ellinger, Y. *J. Phys. Chem.* **1994**, *98*, 9187.

(10) Hudgins, D. M.; Sandford, S. A.; Allamandola, L. J. *J. Phys. Chem.* **1994**, *98*, 4243.

(11) Pauzat, F.; Talbi, D.; Miller, M. D.; DeFrees, D. J.; Ellinger, Y. *J. Phys. Chem.* **1992**, *96*, 7882.

(12) Langhoff, S. R. *J. Phys. Chem.* **1996**, *100*, 2819.

(13) Torii, H.; Sakamoto, A.; Ueno, Y.; Tasumi, M. Manuscript in preparation.

(14) Torii, H.; Furuya, K.; Tasumi, M. *J. Phys. Chem. A* **1998**, *102*, 8422.

(15) Torii, H.; Tasumi, M. *J. Phys. Chem. B* **1997**, *101*, 466.

(16) Torii, H.; Ueno, Y.; Sakamoto, A.; Tasumi, M. *J. Phys. Chem. A* **1999**, *103*, 5557.

(17) Torii, H.; Tasumi, M. *J. Chem. Phys.* **1992**, *97*, 86.

(18) Su, W. P.; Schrieffer, J. R.; Heeger, A. J. *Phys. Rev. B* **1980**, *22*, 2099.

(19) Heeger, A. J.; Kivelson, S.; Schrieffer, J. R.; Su, W.-P. *Rev. Mod. Phys.* **1988**, *60*, 781.

(20) The results obtained for the triphenylene radical cation were given as a preliminary report in Torii, H. *Chem. Phys. Lett.* **1999**, *306*, 381.

(21) Komornicki, A.; McIver, J. W. Jr. *J. Chem. Phys.* **1979**, *70*, 2014.

(22) Shavitt, I. In *Methods of Electronic Structure Theory*; Schaefer, H. F., III, Ed.; Plenum: New York, 1977; Vol. 3, p 189.

(23) Torii, H.; Tasumi, M. *J. Mol. Struct. (THEOCHEM)* **1995**, *334*, 15.

(24) Torii, H.; Tasumi, M.; Bell, I. M.; Clark, R. J. H. *Chem. Phys.* **1997**, *216*, 67.

(25) For part of the cationic species treated in the present study, dipole derivatives in the Cartesian coordinate system were calculated at the B3LYP/6-311G* level in ref 16.

(26) Becke, A. D. *J. Chem. Phys.* **1993**, *98*, 5648.

(27) Lee, C.; Yang, W.; Parr, R. G. *Phys. Rev. B* **1988**, *37*, 785.

(28) Krishnan, R.; Binkley, J. S.; Seeger, R.; Pople, J. A. *J. Chem. Phys.* **1980**, *72*, 650.

(29) Frisch, M. J.; Trucks, G. W.; Schlegel, H. B.; Gill, P. M. W.; Johnson, B. G.; Robb, M. A.; Cheeseman, J. R.; Keith, T.; Petersson, G. A.; Montgomery, J. A.; Raghavachari, K.; Al-Laham, M. A.; Zakrzewski, V. G.; Ortiz, J. V.; Foresman, J. B.; Cioslowski, J.; Stefanov, B. B.; Nanayakkara, A.; Challacombe, M.; Peng, C. Y.; Ayala, P. Y.; Chen, W.; Wong, M. W.; Andres, J. L.; Replogle, E. S.; Gomperts, R.; Martin, R. L.; Fox, D. J.; Binkley, J. S.; Defrees, D. J.; Baker, J.; Stewart, J. J. P.; Head-Gordon, M.; Gonzalez, C.; Pople, J. A. *Gaussian 94*; Gaussian, Inc.: Pittsburgh, PA, 1995.

(30) Coulson, C. A.; Longuet-Higgins, H. C. *Proc. R. Soc. London A* **1947**, *192*, 16.

(31) The phase of each orbital is selected so that positive values of $f_{k,s}$ are obtained for important excited configurations.

(32) Hiratsuka, H.; Hatano, Y.; Tanizaki, Y.; Mori, Y. *J. Chem. Soc., Faraday Trans. 2* **1985**, *81*, 1653.

(33) Rubio, M.; Merchán, M.; Ortí, E.; Roos, B. O. *J. Phys. Chem.* **1995**, *99*, 14980.

(34) Furuya, K.; Torii, H.; Furukawa, Y.; Tasumi, M. *J. Mol. Struct. (THEOCHEM)* **1998**, *424*, 225.